Micromotors

DOI: 10.1002/anie.201103565

A Polymerization-Powered Motor**

*Ryan A. Pavlick, Samudra Sengupta, Timothy McFadden, Hua Zhang, and Ayusman Sen**

Research into nano- and micromotors powered by catalytic reactions, or more broadly the study of autonomous motion at the micro- and nanoscale, has become an area of great current interest.[1] Potential applications include the delivery of materials, self-assembly of superstructures, roving sensors, and other emerging applications. The motors described to date involve the catalytic conversion of small molecules, which typically results in a gradient of charged or neutral species that in turn drives the motor. Polymerization-powered motion has been reported in biological systems, for example, *listeria* has been observed to move by actin polymerization.[2] However, there have been no reports of motion at the nano- and micrometer scale driven by polymerization. Given the large repertoire of known organometallic polymerization catalysts, the design of polymerization-driven motors would considerably increase the scope of catalytic reactions that could be employed to power autonomous motion. Furthermore, polymerization reactions offer the unique opportunity to both power motion and simultaneously allow the deposition of polymer along the motion track.[3] Herein, we present the first motor to be powered by a polymerization reaction outside biological systems. The motor is powered by ring-opening metathesis polymerization (ROMP) of norbornene. These motors show increased diffusion of up to 70% when placed in solutions of the monomer. Furthermore, the motors were observed to display the phenomenon of chemotaxis when placed in a monomer gradient; an extremely rare example outside biology.[4] Generating motion by polymerization has been previously suggested, although not demonstrated.[5]

We chose to employ a form of Grubbs' ROMP catalyst[6] for our initial study because of its relatively high stability and high polymerization activity with norbornene (Figure 1). The motors were fashioned by first synthesizing gold–silica Janus particles. This was performed using 0.96 μm silica particles. These particles were deposited as thin films using a published method.[7] Then gold was deposited onto the monolayers creating the asymmetric Janus particles. The particles were then chemically modified with the Grubbs' catalyst on the silica side utilizing previously published methods (Supporting Information, Figure S1).[8] XPS confirmed that the catalyst did attach to the motor surface. Catalytic activity was then tested by adding the functionalized particles to norbornene solutions and monitoring monomer consumption by gas chromatography. The turnover frequency (TOF) was found to be proportional to monomer concentration and begins to saturate at 1M norbornene (Supporting Information, Figure S2). SEM images of these particles before and after exposure to a monomer solution shows the formation of polymer at the particle surface (Figure 2). As discussed in the Supporting Information, the size increase of the particles owing to polymer formation is not significant under the experimental conditions. Furthermore, this increase would decrease the diffusion coefficient and not increase it as is experimentally observed. The motors were observed using optical microscopy in varying concentrations of monomer in 1,1,1-trichloroethane to study their motion. Note that the formed polymer is freely soluble in this solvent. The particles were tracked over a 10 s period using PhysVis. The diffusion coefficients were extrapolated from the tracking data on about 80 particles by processing with MatLab to generate mean squared displacement (MSD) plots and calculating the slope. Changes in viscosity with different monomer concentrations were taken into account when the diffusion coefficients were computed. This was accomplished by normalizing

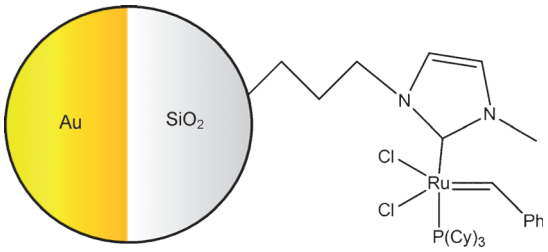

Figure 1. The bound Grubbs' catalyst, shown attached to the silica side of a 0.96 μm gold–silica Janus microsphere.

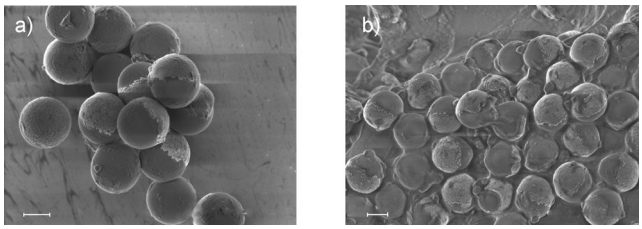

Figure 2. a) SEM image of as-synthesized gold–silica Janus motor particles. b) SEM image of motor particles after exposure to a monomer solution, showing polymer deposition on the motor surface. This deposition is most prevalent on the silica side where the catalyst is bound. Scale bars: 400 nm.

[*] R. A. Pavlick, S. Sengupta, T. McFadden, H. Zhang, Prof. A. Sen
Department of Chemistry, The Pennsylvania State University
University Park, PA 16802 (USA)
E-mail: asen@psu.edu
Homepage: http://research.chem.psu.edu/axsgroup/

[**] This research was supported by Penn State MRSEC (NSF-DMR-0820404) and by the Air Force Office of Scientific Research (FA9550-10-1-0509).

Supporting information for this article is available on the WWW under http://dx.doi.org/10.1002/anie.201103565.

the diffusion coefficients so that the viscosity at each concentration was taken to be the same as that of the pure solvent (Supporting Information, Table S1). Experiments were also done on silica microspheres uniformly coated in Grubbs' catalyst in 0.1 M and 0.5 M norbornene solution. As a control, diffusion of the motor was observed after treatment with an inhibitor, ethyl vinyl ether.

The calculated diffusion coefficients of the motors increased from 0.29 $\mu m^2 s^{-1}$ to 0.49 $\mu m^2 s^{-1}$ going from 0 to 1 M norbornene concentration (Figure 3). This translates to a 70% overall increase in mobility. The increase in diffusion is significantly reduced to 18% when the motors were treated with an inhibitor, which clearly demonstrates that the increase in diffusion stems from substrate turnover. The velocity of the particles also increased from 0.24 $\mu m s^{-1}$ to 0.31 $\mu m s^{-1}$ (Supporting Information, Table S5). For uniformly coated silica particles, the diffusion increase was only 40% compared to 60% for the Janus motor particles in a 0.5 M solution (Supporting Information, Table S6). For the uniformly coated spheres, the increased diffusion is presumably due to small inherent asymmetry or catalysis occurring asynchronously on the sphere surface. Note also that the gold segment is missing in these particles. Thus, the asymmetry of the Janus particle causes an increase in directionality leading to the higher overall increase in diffusion. Furthermore, a plot of the diffusion coefficient versus the natural logarithm of turnover frequency (TOF) revealed a linear relationship between the two (Figure 3). The reason for the observed precise relationship remains unclear. Temporal tracks of the particles reveal that in the presence of monomer the motors exhibit longer linear trajectories and have greater displacements (Figure 4).

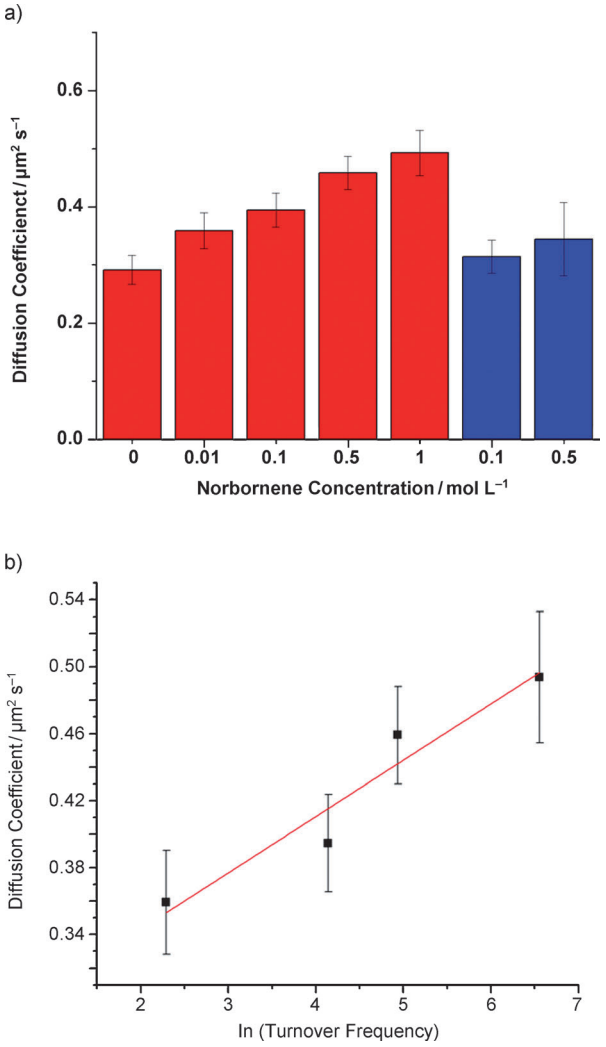

Figure 3. a) Calculated diffusion coefficients of the motor particles at varying monomer concentrations. The diffusion coefficients exhibit a steady increase over the monomer concentrations (red: active). After treatment with an inhibitor, there was a significant decrease in the diffusion coefficient (blue: inhibited), showing that the enhanced diffusion was a result of substrate turnover. b) Plot of the diffusion coefficient versus the natural logarithm of turnover frequency at the same monomer concentration. A linear relationship exists between these two parameters.

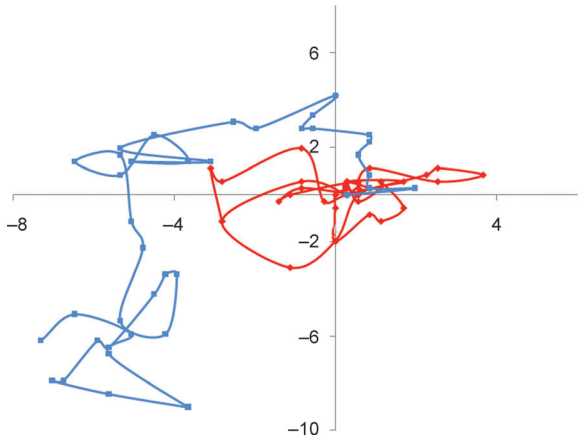

Figure 4. Temporal particle tracks of the motor with no fuel (red) and in 0.5 M norbornene (blue). Each point represents a displacement in μm over 0.5 s, beginning from the origin over a 20 s time span. The motor particles in the fuel show longer displacements in a single direction.

The observed substrate concentration-dependent increase in motor diffusion can be ascribed to osmophoresis.[9] Calculations suggest that an asymmetric catalyst that consumes substrate on one side of the particle and releases either a lower concentration of products and/or a more slowly diffusing product creates an osmotic force across the particle. This force causes net fluid flow from the side with lower substrate concentration (the catalytic side) to the side with higher substrate concentration (the noncatalytic side). The particle will then move in the direction opposite to the fluid flow (Figure 5). In the present case, the asymmetrically placed Grubbs' catalyst consumes many monomer molecules while forming only a few polymer chains, which allows the motor to set up the necessary monomer gradient. Another possible mechanism is a thermal effect. This effect occurs if the reaction is producing enough heat locally to cause an enhancement in the diffusion coefficient. However, our calculations show that at the highest TOF, the temperature change would only be 1.8 μK, which is too small to account for the observed enhancement (Supporting Information). Also, if

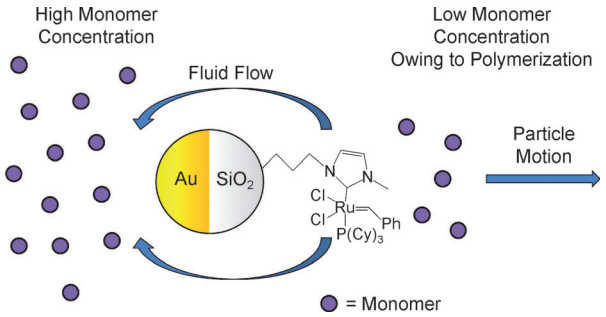

Figure 5. The motor consumes monomers at the silica face, creating an area of low monomer concentration. Fluid in the low concentration region flows towards the higher concentration region at the gold face. Consequently the motor moves in the opposite direction.

the enhanced diffusion was due to a temperature change, the observed diffusion would be directly related to the turnover frequency. Since [Eq. (1)]

$$D = \frac{kT}{6\pi\eta a} \tag{1}$$

where D is the diffusion coefficient, k is the Boltzmann constant, T is temperature, η is viscosity, and a is the particle radius, and the amount of heat released (and thus the local temperature) is directly related to the turnover frequency, therefore [Eq. (2)]

$$D \propto \mathrm{TOF} \tag{2}$$

However, as shown in Figure 3, the diffusion coefficient increase is proportional to the natural logarithm of the TOF.

One of the defining features of living systems is their ability to sense and move up a fuel/food concentration gradient.[10] This phenomenon has very rarely been observed outside biological systems but can form the basis for the design of intelligent sensors that respond to information in the form of gradients. We tested our polymerization motors for their ability to chemotax up a norbornene concentration gradient. A cross-linked acrylate gel containing 1 M norbornene was placed in a solution containing the motor particles. The number of particles at the gel edge was observed over a 4 h period after an initial settling period of 0.5 h. The first observation was taken to be at 0 h. The particle densities were normalized by dividing the number of particles at each time period by the number of particles at 0 h, so that the initial density was taken to be unity (Supporting Information, Table S2). Several runs were averaged together to produce the graph shown in Figure 6. On average, the motor particles increased in concentration at the gel edge with time. After the first hour, the rate of agglomeration began to plateau. This is to be expected, as the concentration gradient of the monomer leaching from the gel is steepest at short times and should begin to level off over longer time spans in accordance with Fick's second law.

To rule out a non-electrolyte diffusiophoretic mechanism for the observed chemotactic behavior, several controls were run. Non-electrolyte diffusiophoresis is a mechanism by

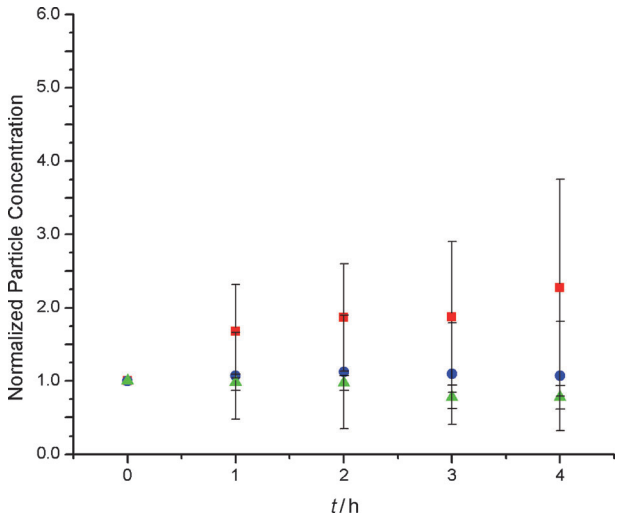

Figure 6. Normalized particle population at the gel edge as a function of time. The populations were normalized so that the initial population is taken to be unity. The motor particles in a norbornene gradient (red) exhibit a higher average agglomeration at the gel over both unfunctionalized gold–silica Janus spheres in a norbornene gradient (blue) and motor particles in a norbornane gradient (green).

which particles move in response to a gradient of an uncharged solute. The velocity is given by Equation (3),

$$U = KL\frac{kT}{\eta}\nabla C \tag{3}$$

where U is the velocity of the particle, K is the Gibbs absorption length, L is the length of the particle–solute interaction, k is the Boltzmann constant, T is temperature, η is viscosity, and C is the solute concentration.[11] If such a mechanism was operating, noncatalytic particles should behave similarly in the presence of the monomer gradient. Accordingly, a control was run with unfunctionalized gold–silica Janus particles in the presence of a norbornene-soaked gel. On average, these particles did not show increased agglomeration at the gel. Another control was run with catalytic motor particles using a norbornane-soaked gel (unlike norbornene, norbornane lacks double-bond functionality and is unreactive). Again, there was no appreciable increase in particle density at the gel over a 4 h period. Therefore it is unlikely that a diffusiophoretic mechanism is behind the observed agglomeration. The control experiments also serve to rule out other noncatalytic advection mechanisms. It should also be noted the particles at the gel edge are not stuck and continue to undergo Brownian-type motion.

The agglomoration of the motor particles at the gel may arise from an enhanced diffusion mechanism as described by Hong et al.[4] The substrate concentration increases continuously as the motor travels up the gradient. Thus, the diffusion rate increases on moving up the gradient and decreases on moving down the gradient. A higher diffusion coefficient results in a higher average displacement causing the motor to move, on average, more towards the gel. This mechanism is absent in the two controls because the particle diffusion coefficient remains relatively constant over the range of

norbornene/norbornane concentrations. The proposed mechanism is stochastic in nature and describes an average trend towards the gel and is different from biological chemotaxis, which requires temporal memory of the concentration gradient. The stochastic nature of the motion is consistent with the observed random trajectories of the motors in the gradient. The observed phenomenon is important as it creates a way to direct the motion of these motors.

In conclusion, a synthetic motor system was designed that exhibits enhanced diffusion by harnessing the energy of a catalytic polymerization reaction. The motor was also found to exhibit the phenomenon of chemtaxis by moving up the monomer gradient. This allows the directed movement of the motor towards specific targets, and should permit the deposition of polymer along the motion track in a solvent in which the polymer is insoluble. Furthermore, the work expands the scope of catalytic reactions that can be utilized to create motion of micrometer-scale objects.

Experimental Section

Grubbs' first-generation catalyst was purchased from Sigma–Aldrich. 3-chloropropyltrimethoxysilane and 1-methylimidazole were purchased from Alfa Aesar. 0.96 μm silica microspheres were purchased from Bangs Laboratories Inc. NMR spectroscopy was performed on a Bruker DPX-300 instrument. GPC was performed on a Shimadzu high-performance liquid chromatograph equipped with a RID-10 A refractive-index detector. XPS spectra were taken on a Kratos Axis Ultra X-ray Photoelectron Spectrometer. Gold and chromium were evaporated in a Semicore E-Beam evaporator. Gas chromatography was accomplished using a Hewlett Packard 5890 Series II Gas Chromatographer. Optical microscopy was performed on a Zeiss Axiovert 200 inverted microscope. The Supporting Information contains experimental methods, synthetic methods, characterization data, activity assays, thermal effects, and raw diffusion and chemotaxis data.

Received: May 24, 2011
Published online: August 30, 2011

Keywords: catalysis · chemotaxis · micromotors · osmophoresis · polymers

[1] a) W. F. Paxton, S. Sundararajan, T. E. Mallouk, A. Sen, *Angew. Chem.* **2006**, *118*, 5546 – 5556; *Angew. Chem. Int. Ed.* **2006**, *45*, 5420 – 5429; b) S. Sanchez, M. Pumera, *Chem. Asian J.* **2009**, *4*, 1402 – 1410; c) J. Wang, K. M. Manesh, *Small* **2010**, *6*, 338 – 345; d) T. Mirkovic, N. S. Zacharia, G. D. Scholes, G. A. Ozin, *Small* **2010**, *6*, 159 – 167; e) Y. Hong, D. Velegol, N. Chaturvedi, A. Sen, *Phys. Chem. Chem. Phys.* **2010**, *12*, 1423 – 1425.
[2] a) M. F. Carlier, S. Wiesner, C. L. Clainche, D. Pantaloni, *C. R. Biol.* **2003**, *326*, 161 – 170; b) H. Watarai, M. Suwa, Y. Iiguni, *Anal. Bioanal. Chem.* **2004**, *378*, 1693 – 1699.
[3] K. M. Manesh, S. Balasubramanian, J. Wang, *Chem. Commun.* **2010**, *46*, 5704 – 5706.
[4] Y. Hong, N. M. K. Blackman, N. D. Kopp, A. Sen, D. Velegol, *Phys. Rev. Lett.* **2007**, *99*, 178103.
[5] J. Godoy, G. Vives, J. M. Tour, *ACS Nano* **2011**, *5*, 85 – 90.
[6] G. C. Vougioukalakis, R. H. Grubbs, *Chem. Rev.* **2010**, *110*, 1746 – 1787.
[7] L. M. Goldenberg, J. Wagner, J. Stumpe, B. R. Paulke, E. Gornitz, *Langmuir* **2002**, *18*, 5627 – 5629.
[8] K. H. Park, S. Kim, Y. K. Chung, *Bull. Korean Chem. Soc.* **2008**, *29*, 2057 – 2060.
[9] a) R. Golestanian, T. B. Liverpool, A. Ajdari, *Phys. Rev. Lett.* **2005**, *94*, 220801 (1-4) ; b) G. Ruckner, R. Kapral, *Phys. Rev. Lett.* **2007**, *98*, 150603 (1-4) ; c) U. M. Córdova-Figueroa, J. F. Brady, *Phys. Rev. Lett.* **2008**, *100*, 158303 (1-4) ; d) H. Ke, S. Ye, R. L. Carroll, K. Showalter, *J. Phys. Chem. A* **2010**, *114*, 5462 – 5467; e) S. Ebbens, R. A. L. Jones, A. J. Ryan, R. Golestanian, J. R. Howse, *Phys. Rev. E* **2010**, *82*, 015304 (1-4) ; f) F. Delogu, *J. Phys. Chem. C* **2009**, *113*, 15909 – 15913.
[10] H. C. Berg, D. A. Brown, *Nature* **1972**, *239*, 500 – 504.
[11] J. L. Anderson, *Annu. Rev. Fluid Mech.* **1989**, *21*, 61 – 99.

